International Journal of Engineering & Technology, 7 (4.14) (2018) 186-190

International Journal of Engineering & Technology

Website: www.sciencepubco.com/index.php/IJET

Research paper

Synthesis and Characterization of MgO Doped ZnO Nanorods Prepared by Solution Immersion Method and their Effect on Energy Band Gap

Z. Khusaimi[1,2*], N.A.M. Asib[1,2], S.Z. Umbaidilah[1,2], A.N. Afaah[1,2], C.N.E. Syafika[2],N.F. Chayed[2,3], M. Rusop[1,4]

[1]NANO-SciTech Centre, Institute of Science,
[2]Faculty of Applied Sciences,
[3] Centre for Nanomaterials Research, Institute of Science
[4]NANO-ElecTronicCentre, Faculty of Electrical Engineering,
Universiti Teknologi MARA, 40450 Shah Alam, Selangor, Malaysia
** Corresponding author E-mail: zurai142@salam.uitm.edu.my*

Abstract

In this research, solid powder form ZnO and MgO-doped ZnO were prepared by using solution immersion method. Mg divalent cation with different atomic percentage of 0.5%, 1.0% and 1.5% were added in 0.04 M of Zn^{2+} solution containing zinc nitrate hexahydrates as precursor and hexamethylene tetraamine as stabilizer. Annealing treatment was consequently carried out to transform the precursors into oxide forms. ZnO and MgO-doped ZnO were successfully obtained and the surface morphology, crystallite size and elemental composition were studied using Field Emission Scanning Electron Microscope (FESEM) and Energy dispersive X-Ray (EDX) respectively. The band gap energy was determined using Ultraviolet-Visible spectrophotometer (UV-Vis). FESEM images showed that the powder form of ZnO and MgO-doped ZnO consist of rod-like shape. A 0.5% of MgO-doped ZnO sample has smallest size of rods with higher aspect ratio compared to others. The EDX result revealed that the sample composed of Zn, O and Mg in the sample. The band gap energy for all samples was determined using Tauc plot and it was found that the band gap energy is reduced with 1.0 and 1.5 % doping while increased at 0.5% doping. The band gap energy was found to range between 3.23 eV to 3.26 eV. The 0.5% of Mg-doped ZnO with higher aspect ratio shows the highest band gap energy value.

Keywords: *undoped ZnO, MgO-doped ZnO, solution immersion method, energy band gap*

1. Introduction

ZnO is a semiconductor which the electrical properties lay between an insulator and conductor. It has wide direct energy bandgap of 3.37 eV and large exciton binding energy of 60 eV [1]. Due to this, it is important to make it attractive for high–temperature electronic and optoelectronic application [1],for example, light emitting diodes (LEDs), UV detectors, and semiconductor laser [2], field emission material [3], gas sensor [4] and transparent conductive coatings [5]. ZnO material also has broad antimicrobial activity which can act against bacteria [6], virus [7] and fungus [8]. Moreover, ZnO is also used in biological application,for example, anti – dandruff shampoo, calamine lotion, baby powder and antiseptic cream [9]

Nowadays, ZnO is one of the materials that have been used in forensic field for fingerprint detection [10-12]. Fingerprint are known as epidermal reliefs that found in the phalanges of each of our fingers which the most useful form of physical evidence in distinguishes all human beings and are unrepeatable. According to Cuce et al., [13], ZnO has been used in white small particle reagents (SPRs) for fingerprint detection. This technique may be observed as a wet powdering method where the detergent solution that contained suspension of fine particle was used in order to visualize latent fingermark. The electromagnetic radiation wavelength of ZnO nanoparticles is about 290 nm and it photoluminescence property emits green and orange light in visible region at 520 nm and 620 nm, respectively[12]. Due to these visible emissions, ZnO nanoparticle is attractive in fingerprint application, where it is needed to form images on dark surfaces by means of UV excitation [14, 15]. Doping is known to modify and deviate the stoichiometry, electrical and optical properties of metal oxides. It has been successfully used to modify energy band gap, improve electron transfer and so affect the optical properties of ZnO that involved its three major luminescence that are ultraviolet (UV) green and red emissions [16].

There are several methods that can be used to synthesize ZnO nanostructure such as spray pyrolysis [17], electrochemical deposition [18], pulsed laser deposition [19] and radio frequency (RF) magnetron sputtering [20]. These methods are described to be capable of producing completely aligned, homogeneously distributed with high crystallinity ZnO. However, high processing temperature are needed and the cost that required for developing is very high [21]. On the other hand, solution-based method has been chosen due to their advantages of synthesizing ZnO nanostructure at much lower cost, lower processing temperature, ease of modifying precursor composition and suitable for large-scale production of ZnO [22]. This method aids the introduction of dopant material during the development of nanostructures [23].

In order to improve the optical and electrical properties of ZnO, doping ZnO with suitable transition element has been chosen [24]. According to previous literature [25], MgO would be an appropri-

ate element that can be used as a dopant in ZnO. This is due to the properties of MgO that has wide energy band gap of 7.80 eV [26] and the substitution of cationic (Mg^{2+}) in ZnO could modified the structural, optical and electrical properties of ZnO [25].

In this work, different concentration of MgO doped ZnO have been synthesized by using solution immersion method and the effect of MgO doped ZnO were characterized by FESEM, EDX and UV-Vis.

2. Experimental

0.04 M of zinc nitrate hexahydrate ($Zn(NO_3)_2.6H_2O$) and hexamethylene tetraamine, (HMTA) ($C_6H_{12}N_4$) solution dissolved in DI water were used to prepare Zn^{2+} solution. 0.5 atomic % (at%) Mg^{2+} solution was prepared by weighing the powder of the $MgNO_3$ and then dissolved in DI water. These prepared solutions were mixed together in molar ratio 1:1. The solution was heated at room temperature for 1 hour at 60 °C and went through aging process for 24 hours with continuous stirring. This solution was then transferred to a glass test-tube and immersed in water bath set at 90 °C for 4 hours. The preparation of Zn^{2+} solution with addition of MgO-doped was repeated to two other concentrations which are 1.0 and 1.5 at%.

The sample then underwent ball milling process conducted at 100 rpm for 1 hour and 100 of zirconia ball was used in order to reduce the particle size of the sample. The sample is formed as a powder after it was centrifuged at 2000 rpm for 2 minutes which separate solid and liquid state of the sample. Lastly, the sample was dried at 120 °C for 20 minutes and followed by annealing process at 500 °C for 1 hour.

The effects of different concentration of MgO-doped to the morphology and transmittance property of ZnO were observed by using FESEM (Carl Zeiss Supra 40 VP) and UV-Vis Spectrophotometer (Perkin Elmer Lambda 950 UV-Vis NIR) respectively. Bang gap energy was consequently calculated from the UV-Vis NIR reflectance spectra by drawing the Tauc plot.

3. Results and Discussion

3.1. Field Emission Scanning Electron Microscope (FE-SEM) Study

The fabricated ZnO powder was analyzed by using FESEM to observe surface morphologies of ZnO at various atomic percent of MgO dopant. Figure 1 (a) to (d) shows the FESEM images of ZnO, 0.5 %, 1.0 % and 1.5 % MgO doped ZnO which, from now on, labeled as ZNO, 0.5ZNO, 1.0ZNO and 1.5ZNO respectively. These micrograph images were measured at 3,000 times magnification and 5.0 kV of voltage. The morphology of ZnO and doped ZnO samples is rod-like shape as shown in Fig. 1.

It also found that the rods have tapered tip at both ends which mostly grown horizontally. The largest ZnO rods were observed in ZnO sample with an average length of 12.84 µm and a diameter of 2.04 µm.

The rods became smaller and shorter as the ZnO was doped at various concentration of MgO. At lowest percentage of doped (0.5ZNO), the sample has smallest size of rods that grown in vertical, inclined and horizontal direction as shown in Figure 1(b). Such arrangement was observed for all doped ZnO samples. The average length and diameter of the rods were 4.56 µm and 0.60 µm. For 1.0ZNO and 1.5ZNO samples, the rods started to increase in diameter and length as observed in Figure 1**(c)** and (d).

The average diameter of 1.0ZNO and 1.5ZNO were 1.84 µm and 1.29µm, respectively. Meanwhile, the average lengths were approximately 9.87 µm and 7.63 µm, respectively. From the measured diameter and length, the aspect ratios of the rods were calculated by dividing the rods length with rods diameter as shown below:

$$\text{Aspect ratio: } \frac{\text{Length of rods } (\mu m)}{\text{Diameter of rods } (\mu m)}$$

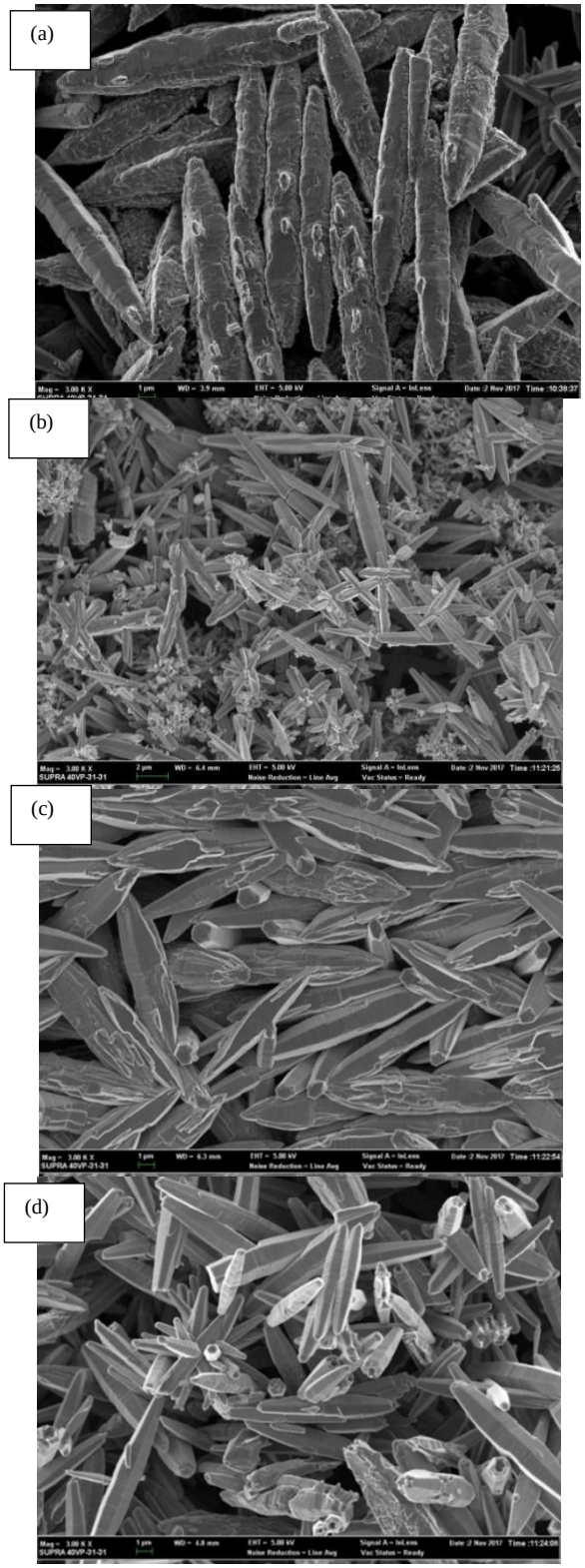

Fig. 1: FESEM images of (a) ZNO, (b) 0.5ZNO, (c) 1.0ZNO and (d) 1.5ZNO.

The obtained aspect ratios were listed in Table 1. These values of aspect ratios varied from 5.36 to 7.60. Interestingly, 0.5ZNO has the highest aspect ratio of 7.60 compared to the other samples. A higher aspect ratio indicates thinner rods. The reduction of rods size at lowest concentration of MgO-dopant attributed to the moderate amount of doping which promote the growth of crystal plane and assist dopant atoms to be orderly incorporated into a ZnO

lattice. In contrast, excess doping restricts the function of the dopant in the ZnO [27, 28].

Table 1: The average length, diameter and aspect ratio for all samples.

Samples	Average Length (µm)	Average Diameter (µm)	Aspect ratio
ZNO	12.84	2.04	6.29
0.5ZNO	4.56	0.60	7.60
1.0ZNO	9.87	1.84	5.36
1.5ZNO	7.63	1.29	5.91

3.2. Energy Dispersive X-ray (EDX) Study

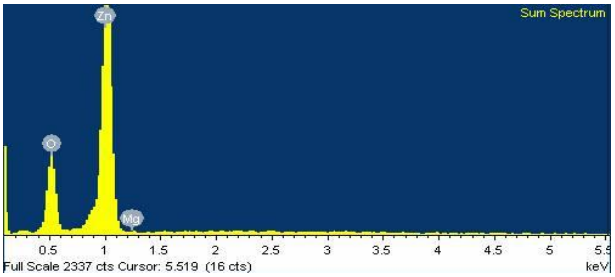

Fig 2: The EDX spectrum of ZnO doped with 0.5% of MgO (0.5ZNO) sample.

The elemental composition of 0.5ZNO sample is confirmed by EDX analysis which revealed the presence of elements Zn, O and Mg as can be observed in Figure 2.The EDX data of weight % and atomic % for each element in 0.5ZNO sample are listed in Table 2. The presence of Mg considered to be 0.5% exhibited 0.66% instead from the EDX result, is suggested to be due to indeterminate error.

Table 2: EDX data of elemental composition of 0.5ZNO sample.

Element	Weight (%)	Atomic (%)
O	21.07	51.96
Mg	0.41	0.66
Zn	78.52	47.39

3.3. Band gap studies using UV-VIS Spectrophotometer

The samples were analysed using UV-Vis-NIR spectrophotometer to determine the band gap energy of each sample. Figure 3 represents the transmittance spectra of ZnO and MgO-doped ZnO in the wavelength range of 200-1600 nm. The absorption edges were ~400 nm for ZnO and MgO-doped ZnO samples. From the figure, the samples revealed a high transparency with over 90% for ZNO, 1.0ZNO and 1.5ZNO in the visible and near-infra-red region. Meanwhile the transparency of 0.5ZNO is the lowest which is about 80% in the visible and near-infra-red region. This result supported the FESEM findings which affiliate with the trend provided by the sample of 0.5ZNO. Having thinner rods lead to lower transparency and so higher absorption or reflectance capability.

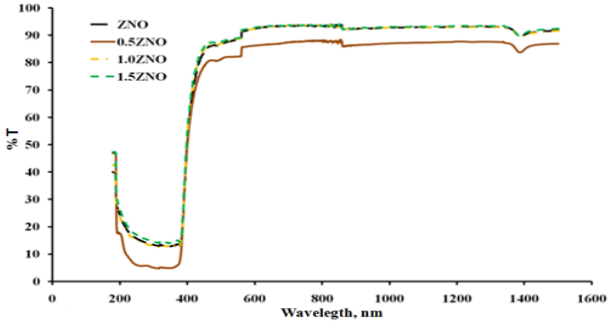

Fig. 3: UV–VIS–NIR transmittance against photon wavelength of ZNO, 0.5ZNO, 1.0ZNO, 1.5ZNO samples

The reflectance spectrum of ZnO and Mg-doped ZnO was shown in Fig. 4. All of the samples show that the reflectance is increasing from UV to visible range with more than 80% of reflectance. Equally as in the transmittance spectrum in Figure 3, sample 0.5ZN reflectance is overriding the others.

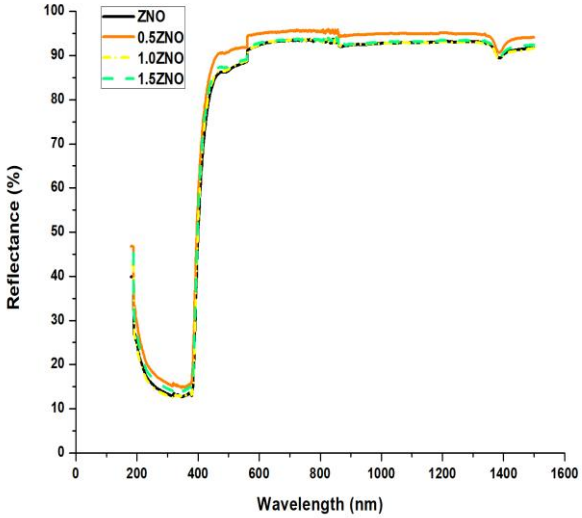

Fig. 4: The reflectance spectrum of (a) ZNO, (b) 0.5ZNO, (c) 1.0ZNO and (d) 1.5ZNO

The band gap energy, E_g, values of the samples can be obtained from the Tauc plot that is derived from the equation below [29]. The absorption edge for direct inter-band transition is given by relations (1) and (2) below;

$$(\alpha hv)^2 = A(hv - E_g) \quad (1)$$

$$A = k\, ln\, \frac{(Rmax - Rmin)}{R - Rmin} \quad (2)$$

where α is the absorption coefficient of the material, *A* is the energy-independent constant with values between 1 x 10^5 and 1 x 10^6 cm^{-1} eV^{-1}, *hv* is the photon energy and E_g is the optical band gap energy. The Tauc plot can be drawn from $(\alpha hv)^2$ versus *hv*. The band gap energy of the samples was determined from extrapolation of the linear part that intercepts the photon energy axis.

The Tauc plot of all samples are shown in Figure 5. From the Tauc plot, the band gap energy of the samples is found to be between 3.23 eV to 3.26 eV as tabulated in Table 3. The presence of dopant causes the changes in the band gap energy which modifying the energy level [28]. It is observed that the increase of concentration of MgO dopant in ZnO resulted in a decrease of band gap energy. The 0.5ZNO sample exhibit the highest value of band gap energy which is 3.26 eV whereas 1.5ZNO sample exhibit the smallest band gap energy with the value of 3.23 eV. This is due to the effect of crystallite size on the band gap energy. Band gap widening of the samples are attributed to the quantum mechanical effects of the low-dimensional crystallites.The higher band gap energy is due to the smaller size of sample. The higher aspect ratio caused by the thinner rods affect the energy levels that can widen the band.

Table 3: The band gap energy ZNO, 0.5ZNO, 1.0ZNO, 1.5ZNO samples

Samples	Band gap energy (eV)
ZNO	3.25
0.5ZNO	3.26
1.0ZNO	3.24
1.5ZNO	3.23

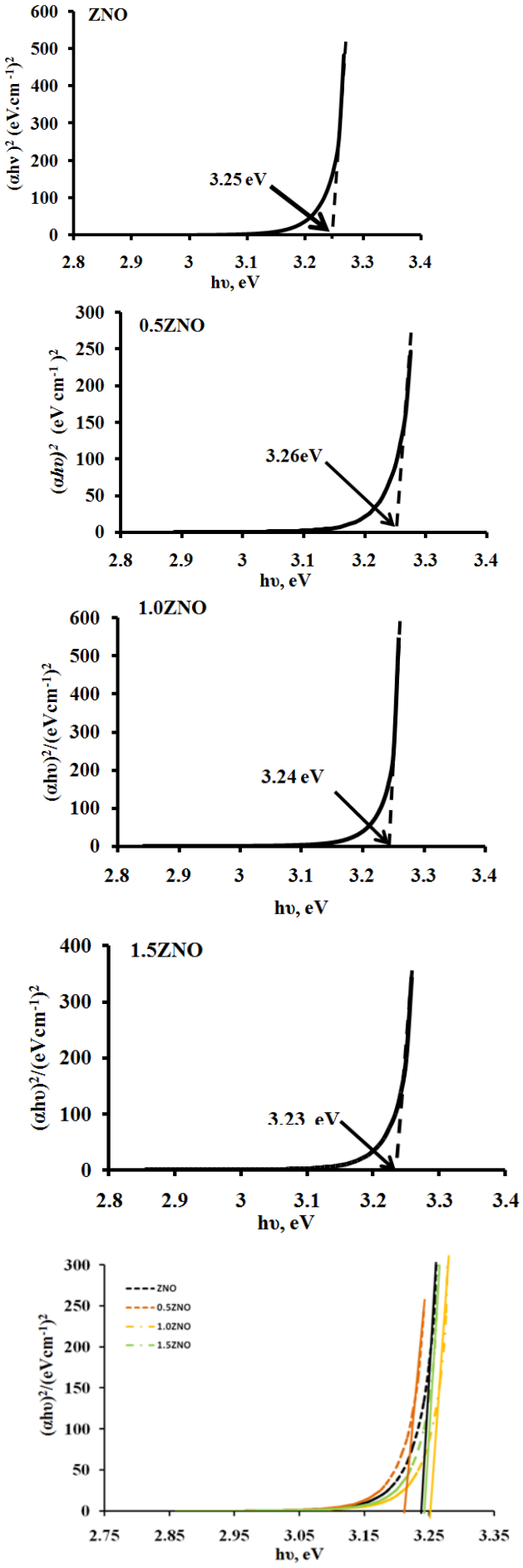

Fig. 5: Tauc plot of ZNO, 0.5ZNO, 1.0ZNO, 1.5ZNO samples and a combination of the four spectrum

4. Conclusion

A rod-like shape of ZnO and MgO-doped ZnO were successfully synthesized at 90 °C water bath temperature of solution immersion method followed by 500 °C annealing temperature. The existence of the same rod-like structure in all % of MgO shows that the growths of the sample were independent of the MgO presence. However, its presence does affect the diameter and length of ZnO rods with 0.5ZNO produced the highest aspect ratio. The band gap energy of ZnO and MgO-doped ZnO has values between 3.23 eV to 3.26 eV. The 0.5ZNO sample with higher aspect ratio exhibited highest band gap energy of 3.26 eV. As a conclusion, the presence of MgO dopant has modified the energy levels and the band gap energy of ZnO.

Acknowledgement

We would like to express our gratitude to Ministry of Education Malaysia, Research Management Institute and UniversitiTeknologi MARA (UiTM), Shah Alam, Selangor, Malaysia for financial support.

References

[1] V. Coleman and C. Jagadish, "Basic properties and applications of ZnO," *Zinc Oxide Bulk, Thin Films and Nanostructures: Processing, Properties, and Applications*, pp. 1-20, 2006.

[2] J. Hassan, M. Mahdi, A. Ramizy, H. A. Hassan, and Z. Hassan, "Fabrication and characterization of ZnO nanorods/p-6H–SiC heterojunction LED by microwave-assisted chemical bath deposition," *Superlattices and Microstructures*, vol. 53, pp. 31-38, 2013.

[3] F. Jamali-Sheini, R. Yousefi, M. A. More, and D. S. Joag, "Sn–ZnO nanoneedles grown on Zn wire as a pointed field emitter and switching device," *Materials Letters*, vol. 111, pp. 181-184, 2013.

[4] Q. Ahsanulhaq, J. Kim, J. Lee, and Y. Hahn, "Electrical and gas sensing properties of ZnO nanorod arrays directly grown on a four-probe electrode system," *Electrochemistry Communications*, vol. 12, pp. 475-478, 2010.

[5] T. Minami, "Transparent and conductive multicomponent oxide films prepared by magnetron sputtering," *Journal of Vacuum Science & Technology A*, vol. 17, pp. 1765-1772, 1999.

[6] L. Zhang, Y. Jiang, Y. Ding, M. Povey, and D. York, "Investigation into the antibacterial behaviour of suspensions of ZnO nanoparticles (ZnO nanofluids)," *Journal of Nanoparticle Research*, vol. 9, pp. 479-489, 2007.

[7] J. You, Y. Zhang, and Z. Hu, "Bacteria and bacteriophage inactivation by silver and zinc oxide nanoparticles," *Colloids and Surfaces B: Biointerfaces*, vol. 85, pp. 161-167, 2011.

[8] A. Lipovsky, Y. Nitzan, A. Gedanken, and R. Lubart, "Antifungal activity of ZnO nanoparticles—the role of ROS mediated cell injury," *Nanotechnology*, vol. 22, p. 105101, 2011.

[9] O. Akhavan and E. Ghaderi, "Enhancement of antibacterial properties of Ag nanorods by electric field," *Science and Technology of Advanced Materials*, vol. 10(1), p. 015003, 2016.

[10] N. H. Deepthi, R. B. Basavaraj, S. C. Sharma, J. Revathi, Ramani, S. Sreenivasa, and H. Nagabhushana, "Rapid visualization of fingerprints on various surfaces using ZnO superstructures prepared via simple combustion route," *Journal of Science: Advanced Materials and Devices*, vol. 3, pp. 18-28, 2018.

[11] M. Zhang, G. Qin, Y. Zuo, T. Zhang, Y. Zhang, L. Su, H. Qiu, and X. Zhang, "SECM imaging of latent fingerprints developed by deposition of Al-doped ZnO thin film," *Electrochimica Acta*, vol. 78, pp. 412-416, 2012.

[12] M. Guzman, B. Flores, L. Malet, and S. Godet, "Synthesis and Characterization of Zinc Oxide Nanoparticles for Application in the Detection of Fingerprints," *Materials Science Forum*, vol. 916, pp. 232-236, 2018.

[13] P. Cuce, G. Polimeni, A. Lazzaro, and G. De Fulvio, "Small particle reagents technique can help to point out wet latent fingerprints," *Forensic science international*, vol. 146, pp. S7-S8, 2004.

[14] T. Andelman, Y. Gong, M. Polking, M. Yin, I. Kuskovsky, G. Neumark, and S. O'Brien, "Morphological control and photoluminescence of zinc oxide nanocrystals," *The Journal of Physical Chemistry B*, vol. 109, pp. 14314-14318, 2005.
[15] P. Taunk, R. Das, D. Bisen, and R. kumar Tamrakar, "Structural characterization and photoluminescence properties of zinc oxide nano particles synthesized by chemical route method," *Journal of Radiation Research and Applied Sciences*, vol. 8, pp. 433-438, 2015.
[16] S. Zhao, Y. Zhou, K. Zhao, Z. Liu, P. Han, S. Wang, W. Xiang, Z. Chen, H. Lü, B. Cheng, and G. Yang, "Violet luminescence emitted from Ag-nanocluster doped ZnO thin films grown on fused quartz substrates by pulsed laser deposition," *Physica B: Condensed Matter*, vol. 373, pp. 154-156, 2006/03/01/ 2006.
[17] U. Alver, T. Kılınç, E. Bacaksız, T. Küçükömeroğlu, S. Nezir, I. Mutlu, and F. Aslan, "Synthesis and characterization of spray pyrolysis Zinc Oxide microrods," *Thin Solid Films*, vol. 515, pp. 3448-3451, 2007.
[18] R. Chander and A. Raychaudhuri, "Electrodeposition of aligned arrays of ZnO nanorods in aqueous solution," *Solid State Communications*, vol. 145, pp. 81-85, 2008.
[19] M. Rusop, K. Uma, T. Soga, and T. Jimbo, "Post-growth annealing of zinc oxide thin films pulsed laser deposited under enhanced oxygen pressure on quartz and silicon substrates," *Materials Science and Engineering: B*, vol. 127, pp. 150-153, 2006.
[20] R. Navamathavan, S.-J. Park, J.-H. Hahn, and C. K. Choi, "A nanoindentation analysis of the influence of lattice mismatch on some wide band gap semiconductor films," *Physica B: Condensed Matter*, vol. 403, pp. 675-678, 2008.
[21] K. Gautam, I. Singh, P. K. Bhatnagar, and K. R. Peta, "The effect of growth temperature of seed layer on the structural and optical properties of ZnO nanorods," *Superlattices and Microstructures*, vol. 93, pp. 101-108, 2016.
[22] T. Touam, F. Boudjouan, A. Chelouche, S. Khodja, M. Dehimi, D. Djouadi, J. Solard, A. Fischer, and A. Boudrioua, "Effect of silver doping on the structural, morphological, optical and electrical properties of sol–gel deposited nanostructured ZnO thin films," *Optik-International Journal for Light and Electron Optics*, vol. 126, pp. 5548-5552, 2015.
[23] N. A. Abdullah, Z. Khusaimi, and M. Rusop, "A Review on Zinc Oxide Nanostructures: Doping and Gas Sensing," *Advanced Materials Research*, vol. 667, pp. 329-332, 2013.
[24] I. Khan, S. Khan, R. Nongjai, H. Ahmed, and W. Khan, "Structural and optical properties of gel-combustion synthesized Zr doped ZnO nanoparticles," *Optical Materials*, vol. 35, pp. 1189-1193, 2013.
[25] Q. A. H. Al-Naser, J. Zhou, H. Wang, G. Liu, and L. Wang, "Synthesis and optical properties of MgO-doped ZnO microtubes using microwave heating," *Optical Materials*, vol. 46, pp. 22-27, 2015.
[26] H.-C. Hsu, C.-Y. Wu, H.-M. Cheng, and W.-F. Hsieh, "Band gap engineering and stimulated emission of ZnMgO nanowires," *Applied Physics Letters*, vol. 89, p. 013101, 2006.
[27] K. Verma, B. Chaudhary, V. Kumar, V. Sharma, and M. Kumar, "Investigation of structural, morphological and optical properties of Mg: ZnO thin films prepared by sol-gel spin coating method," *Vacuum*, vol. 146, pp. 524-529, 2017/12/01/ 2017.
[28] Y. Liu, H. N. Liu, Y. Yu, and Z. Wang, "Effects of Cu doping on the surface morphology, microstructure and photoluminescent characteristics of ZnO films," *Materials Research Innovations*, vol. 19, pp. S8-798-S8-801, 2015/11/01 2015.
[29] L. Cao, L. Zhu, and Z. Ye, "Enhancement of p-type conduction in Ag-doped ZnO thin films via Mg alloying: The role of oxygen vacancy," *Journal of Physics and Chemistry of Solids*, vol. 74, pp. 668-672, 2013.